Theor Chim Acta (1993) 86: 241–248

Theoretica Chimica Acta

Dynamics of the H + LH′ reaction Cl + HBr → HCl + Br. TST-CEQ and VTST calculations

Bian Wen-Sheng and Ju Guan-Zhi
Institute of Theoretical Chemistry, Shandong-University, 250100, Jinan, P.R. China

Received February 5, 1992/Accepted January 5, 1993

Summary. Collinear quantum scattering calculations have been carried out using hyperspherical coordinates and the Broida–Persky LEPS surface for the title reaction. Our results are compared with those from available similar calculations. We have also calculated some state-selected reaction cross sections and rate constants by the method of TST-CEQ, and these are found to be close to previous QCT and experimental results. VTST calculations are also done on the same surface and the calculated thermal rate constants and kinetic isotope effects are in good agreement with those from QCT calculations and experiments. We conclude that the potential energy surface used in the present study may be a better one and is recommended to be employed in further dynamical calculations.

Key words: Cross sections – Quantum scattering – ClHBr – TST-CEQ – Rate constants

1 Introduction

Several studies on the dynamics of the reaction Cl + HBr have been reported [1–14]. Almost all the theoretical work has been based on semi-empirical potential energy surfaces [1, 6–14], particularly extended-LEPS surfaces, but it has not been clear which of the various surfaces used is the best one. Recently, Persky and Broida have adjusted a LEPS surface based on their 3-D quasiclassical trajectory calculations, which was found to reproduce quite well the experimental rate constant and product energy distributions [1]. Therefore, some additional calculations on this newly-adjusted surface should be of interest.

Over six years ago, some collinear quantum scattering studies for the ClHBr system were done on several semi-empirical surfaces [9–14]. In the present work we did collinear quantum scattering calculations for an additional surface, in particular the Broida–Persky LEPS surface [1], which has almost no barrier. Then we converted the collinear reaction probabilities into 3-D cross sections and rate constants using the TST-CEQ (transition-state-theory-collinear-exact-quantum) method [15, 16], which make it possible to compare our results with the QCT (quasi-classical-trajectory) and experimental ones. VTST (variational-

transition-state-theory) calculations have also been carried out, which may be the first-presented results of its kind for the 3-D Cl + HBr reaction in the literature.

2 Computational methods

The collinear reaction probabilities are obtained using the hyperspherical coordinate method, as described previously [17]. Our programs applying this method have been verified through calculations on the model system F + H2. In the present calculations, eight basis functions are used and two closed channels are retained to guarantee the convergence of probabilities. The maximum error is estimated to be less than 0.01.

The TST-CEQ method was first proposed by Bowman and G.Z. Ju [15]. It incorporates collinear quantum reaction probabilities into transition-state theory and yields state-selected cross sections and rate constants. The details of this method may be found in our recent work [16]. Calculations based on this method are performed through program written by us.

The variational transition-state theory (VTST) calculations are accomplished by applying the Polyrate Scientific Program [18]. In the course of our calculations, variable-step Adams–Moulton fourth-order integrator is used along the minimum energy path, mode analysis is performed every $0.02\,a_0$ step, and MorseIa is chosen for the calculation of vibrational energy levels.

All above calculations are conducted on the FACOM M-340s machine of Shandong University.

3 Potential energy surface

Since an *ab initio* PES is unavailable for the reaction Cl + HBr, semi-empirical, particularly extended-LEPS, surfaces were used in previous various dynamical calculations [1, 6–14]. These surfaces differ in barrier height and other features, and it is unclear which is best.

The PES employed in the present study was proposed by Persky et al. [1] about two years ago. Of the many surfaces examined [1], this one gives the best agreement with experimental kinetic data. It has a very low barrier (about 0.30 kcal/mol) located very early in the entrance valley. All the related parameters for this surface can be found in [1]. Our calculations on this surface may help to assess this surface.

4 Results and discussion

4.1 The collinear reaction probabilities

P^R_{02}, P^R_{13}, P^R_{03} and P^R_{12} are shown in Figs. 1(a–d) as functions of total energy measured from the bottom of the HBr well. The first subscript denotes the vibrational quantum number of HBr, and the second denotes that for HCl. The other state-to-state reaction probabilities are small (generally less than 0.05) and are not presented. From Figs. 1(a–d), we can summarize some features of the reaction probabilities as follows:

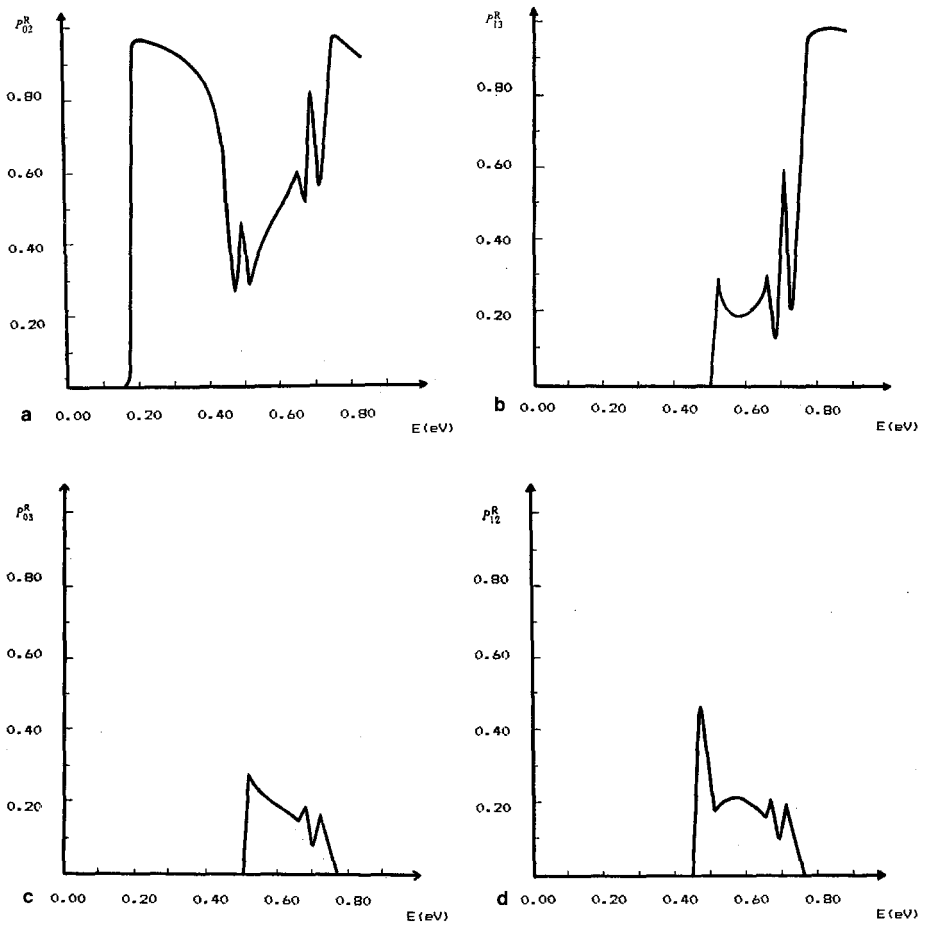

Fig. 1. **a** Reactive probabilities versus total energy E. **b** Reactive probabilities versus total energy E. **c** Reactive probabilities versus total energy E. **d** Reactive probabilities versus total energy E

1) The reaction probabilities P^R_{02} and P^R_{13} are largest. The energy levels of the reactant (HBr) for the vibrational states $v = 0, 1$ are near to those of the product (HCl) for $v = 2, 3$ respectively, so the above results indicate that the reaction probabilities between the two nearly degenerate states are dominant. This phenomenon results from the conservation of translational energy of the HLH system [9] and is also observed in Refs. [10–14].

2) The reaction probabilities all exhibit some oscillations. These oscillations can be attributed to dynamic (Feschbach) resonances [12]. Dynamic resonances were discussed previously in many papers [19].

3) From Figs. 1(a) we can see that, the threshold energy of the reactive transition $v = 0 \rightarrow v = 2$ (about 0.163 eV) is only a little higher than the zero point vibrational energy of the reactant HBr (about 0.1628 eV). This may come from the very low barrier height (0.3 kcal/mol) of the reaction. The barrier height of the PES used in Ref. [10] is 1 kcal/mol, and the corresponding

threshold energy is 0.19 eV. Ref. [12] employed a high barrier (about 12 kcal/mol) LEPS surface, and the corresponding threshold energy becomes 0.43 eV. So the increase of the barrier height of the PES raises the reactive threshold energy, which is reasonable.

4) As far as the non-adiabatic probabilities (such as P_{03}^R, P_{12}^R, P_{01}^R, and P_{11}^R) are concerned, we find some differences from Refs. [10] and [12], in which all the non-adiabatic probabilities for various transitions are within the range 0.01–0.10 and are near to one another. Our results (see Figs. 1(c) and (d)) show that P_{03}^R and P_{12}^R are a little more favored.

4.2 TST-CEQ calculations

4.2.1 Average state-selected cross sections $\overline{Q}^{TST-CEQ}(E, v)$. On the basis of the above data for the state-to-state collinear reaction probabilities, we have obtained the 3-D state-selected reaction cross sections through the TST-CEQ method, and these are displayed in Fig. 2.

First, Fig. 2 shows that the $\overline{Q}^{TST-CEQ}(E, v)$ curves increase continuously with total energies without any oscillating behaviour such as is observed in the figures of the collinear probabilities (see Sect. 4.1). In this point, our results are in agreement with Persky et al. [1].

Secondly, $Q(E, 1)$ is larger than $Q(E, 0)$ at higher energies. This means that the vibrational energy is more effective than translational energy in promoting the reaction Cl + HBr. It is usually expected that translational energy should be more effective for systems with early barriers [25], but for the H + LH′ class of reactions, whether they have a late barrier or an early one, vibrational energy is found to be more effective [1, 20–22], because of the small skew angle [1] between the reactants and products valley of the potential energy surface in mass-scaled coordinates.

Finally, we'd like to compare our results for cross sections with Ref. [1] in some detail. The reactive threshold energies shown in Fig. 2 are about 0.18 eV for $v = 0$ and 0.50 eV for $v = 1$, whereas those of Ref. [1] are around 4 kcal/mol (0.173 eV) and 11.2 kcal/mol (0.486 eV) correspondingly. So only a little differ-

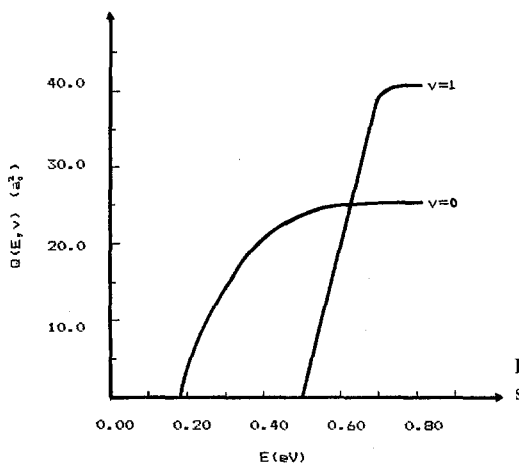

Fig. 2. TST-CEQ average reaction cross sections versus the total energy E

ence is found between them. Figure 2 also shows that, the values of the state-selected cross section stabilize at $25.5\,a_0^2$ (7.14 Å^2) for $v = 0$ and $40\,a_0^2$ (11.20 Å^2) for $v = 1$, when the total energy E is high. These values are several times bigger than those (2.2 Å^2 and 4.0 Å^2 respectively) of Ref. [1].

4.2.2 State-selected rate constants $k^{TST-CEQ}(T, v)$. We have also calculated the reactive rate constants for the specified vibrational state ($v = 0, 1$) using the TST-CEQ method, and our results are summarized in Fig. 3.

From Fig. 3 we can see that, $\log(k(v))$ increases smoothly when the temperature rises, but the empirical Arrhenius behaviour is not well followed, and the curve of $k(0)$ is very close to that of $k(1)$, which can be explained by the very low barrier of the reaction Cl + HBr. Figure 3 also shows that, at higher temperatures, $k(1)$ gets a little smaller than $k(0)$, but the difference between them is within the range of errors that may be involved in our 1-D quantum mechanical and TST-CEQ calculations.

The calculated rate constants are in agreement with those of QCT [1]. For example, at 300 K, the TST-CEQ rate constant for $v = 0$ is 3.2×10^{-12} cm$^3 \cdot$ molecule$^{-1} \cdot$ sec^{-1}, and that from QCT is 8.1×10^{-12} cm$^3 \cdot$ molecule$^{-1} \cdot$ sec^{-1}; at 500 K, the TST-CEQ rate constant for $v = 0$ is 1.05×10^{-11} cm$^3 \cdot$ molecule$^{-1} \cdot$ sec^{-1}, whereas that from QCT is 1.58×10^{-11} cm$^3 \cdot$ molecule$^{-1} \cdot$ sec^{-1}. So at higher temperatures, the agreement becomes better.

4.3 VTST calculations

We have performed some VTST calculations for the reactions Cl + HBr and Cl + DBr; previously [14] VTST results for the collinear Cl + HBr reaction were reported. All the related results are included in Tables 1 and 2, in which $\neq$, CVT and ICVT denote conventional transition state theory, canonical variational transition state theory, and improved canonical variational transition state theory respectively, and $\neq/W$ and MEPSAG have the same meaning as the literature [23]. In particular, W denotes the Wigner tunneling correction and

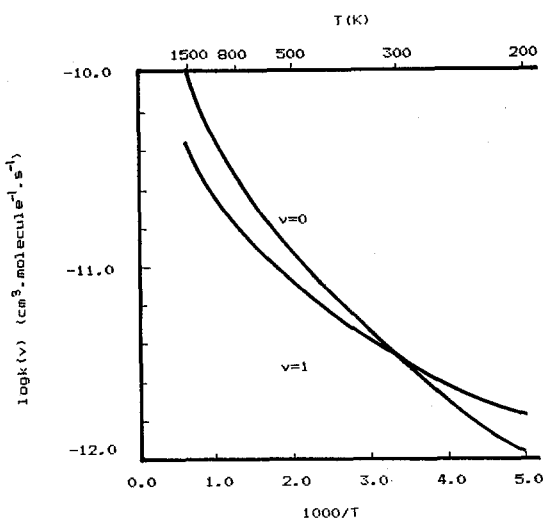

Fig. 3. Arrhenius plot of the TST-CEQ state-selected thermal rate constant

Table 1. The tunneling factors

T (K)	$\neq/W$	MEPSAG	CVT/CAG	$\neq/W$	MEPSAG	CVT/CAG
		Cl + HBr			Cl + DBr	
200	1.004	1.181	1.000	1.004	1.535	0.986
300	1.002	1.079	1.000	1.002	1.227	0.991
600	1.000	1.019	1.000	1.000	1.055	0.995
1000	1.000	1.007	1.000	1.000	1.020	0.997
1500	1.000	1.003	1.000	1.000	1.009	0.998

Table 2. The various calculated rate constants ($cm^3 \cdot molecule^{-1} \cdot sec^{-1}$)

T (K)	$\neq$	$\neq/W$	CVT	CVT/MEPSAG	ICVT	ICVT/MEPSAG
Cl + HBr						
200.0	5.52(−12)	5.54(−12)	5.52(−12)	6.52(−12)	5.52(−12)	6.52(−12)
300.0	1.02(−11)	1.02(−11)	1.02(−11)	1.10(−11)	1.02(−11)	1.10(−11)
600.0	2.84(−11)	2.84(−11)	2.84(−11)	2.89(−11)	2.84(−11)	2.89(−11)
1000.0	6.10(−11)	6.10(−11)	6.10(−11)	6.14(−11)	6.10(−11)	6.14(−11)
1500.0	1.14(−10)	1.14(−10)	1.14(−10)	1.14(−10)	1.14(−10)	1.14(−10)
Cl + DBr						
200.0	4.46(−12)	4.48(−12)	4.46(−12)	6.75(−12)	4.46(−12)	6.84(−12)
300.0	8.73(−12)	8.73(−12)	8.72(−12)	1.06(−11)	8.72(−12)	1.07(−11)
600.0	2.61(−11)	2.61(−11)	2.61(−11)	2.74(−11)	2.61(−11)	2.75(−11)
1000.0	5.83(−11)	5.83(−11)	5.83(−11)	5.93(−11)	5.83(−11)	5.95(−11)
1500.0	1.11(−10)	1.11(−10)	1.11(−10)	1.12(−10)	1.11(−10)	1.12(−10)

MEPSAG denotes the minimum-energy-path semi-classical adiabatic ground-state tunneling correction. The SCSAG (small curvature semi-classical adiabatic ground-state) tunneling correction was not able to be carried out because of the small skew angle for the ClHBr mass combination. (The more appropriate LCG3 or LAG [24] correction, either of which is suitable for the HLH mass combination, has not been included in our program.) However the tunneling contribution appears to be small (see Table 1).

From Table 2 we see that our VTST rate constants are in agreement with those of Ref. [1] for the reaction Cl + HBr. For example, at 300 K, the rate constant from ICVT/MEPSAG is 1.10×10^{-11} $cm^3 \cdot molecule^{-1} \cdot sec^{-1}$, whereas that from QCT is about 8.1×10^{-12} $cm^3 \cdot molecule^{-1} \cdot sec^{-1}$; at 500 K the rate constant from ICVT/MEPSAG is about 2.24×10^{-11} $cm^3 \cdot molecule^{-1} \cdot sec^{-1}$, whereas that from QCT is something a little more than 1.58×10^{-11} $cm^3 \cdot molecule^{-1} \cdot sec^{-1}$. When D replaced H in the reaction Cl + HBr, some decrease is observed for all kinds of rate constants listed in Table 2, and the QCT [1] results also show us this kind of kinetic isotope effect. So agreement with QCT is obtained for kinetic isotope effects as well.

4.4 Comparison of various thermal rate constants

The TST-CEQ state-selected rate constants are averaged to yield the thermal rate constants, which are plotted in Fig. 4, and for the sake of a clear comparison, the

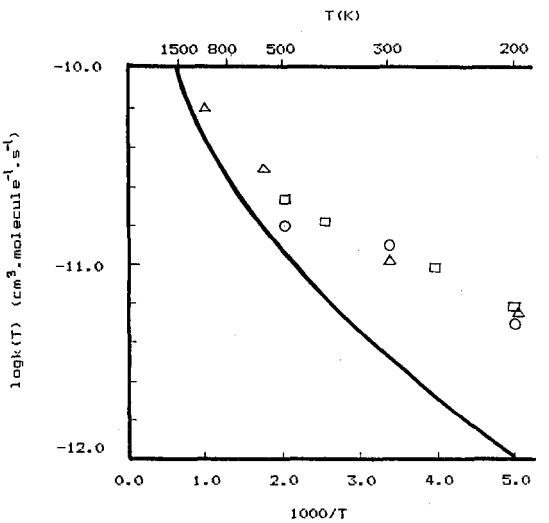

Fig. 4. Comparison of different kinds of thermal rate constants. The *solid curve* is present work. *Triangles*, *circles* and *squares* are from ICVT/MEPSAG calculations. QCT calculations and experiments respectively [1]

results from VTST and QCT calculations, and some experiments [1] are also placed in it. It is shown that, at higher temperatures, the various results are in good agreement with one another, but when the temperature goes down, those of TST-CEQ diverge towards lower values. We think that this kind of divergency may come from the TST-CEQ approximation. More tunneling may occur in 3D than is predicted by the use of the TST-CEQ extension from 1D to 3D, leading to the fact that the TST-CEQ model underestimated the rate constants for the reaction Cl + HBr at lower temperatures. We hope we can improve this in the future.

5 Conclusions

The quantum mechanical structures of the collinear reaction probabilities for Cl + HBr($v \leqslant 1$) → HCl($v' \leqslant 3$) + Br on a LEPS surface with a very low barrier are presented, and qualitative agreement is found when these results are compared with previous ones on some other semi-empirical surfaces [10–14].

Our TST-CEQ calculations have yielded some useful results. The calculated average reactive cross sections do not exhibit oscillatory behaviour and indicate that vibrational energy is more effective than translational energy for the title reaction. The calculated state-selected rate constants increases smoothly when the temperature T rises, but the empirical Arrhenius behaviour is not well followed. Furthermore, the calculated values of the above cross sections and rate constants are close to those found in Ref. [1].

Some VTST calculations are accomplished for the title reaction and the kinetic isotope effect is also considered. When the obtained results are compared with QCT calculations and experiments, good agreement is observed.

It is encouraging to see that various results from different dynamical theoretical calculations and experiments, are in reasonable agreement with one another. This may indicate that the Broida–Persky LEPS surface used in the present calculations provides a better physical approximation to the true surface.

Acknowledgments. We are indebted to Professor Deng Cong-Hao and Chen De-Zhan for helpful discussions.

References

1. Broida M, Persky A (1989) Chem Phys 133:405
2. Mei CC, Moore CB (1977) J Chem Phys 67:3936
3. Rubin R, Persky A (1983) J Chem Phys 79:4310
4. Lamb JJ, Benson SW (1986) J Phys Chem 90:941
5. Dolson DA, Leone SR (1987) J Phys Chem 91:3543
6. Douglas DJ, Polanyi JC, Sioan JJ (1976) Chem Phys 13:15
7. Brown JC, Bass HE, Thompson DL (1977) J Phys Chem 81:479
8. Smith JWM (1977) Chem Phys 20:437
9. Baer M (1975) J Chem Phys 62:305
10. Kaye JA, Kuppermann A (1982) Chem Phys Lett 92:574
11. Babamov VK, Marcus RA (1983) Chem Phys Lett 101:507
12. Abu-Salbi N, Kouri DJ, Lopez V, Babamov VK, Marcus RA (1984) Chem Phys Lett 103:458
13. Lopez V, Babamov VK, Marcus RA (1984) J Chem Phys 81:3962
14. Garrett BC, Abu-Salbi N, Kouri DJ, Truhlar DG (1985) J Chem Phys 83:2252
15. Bowman JM, Ju GZ, Lee KT (1982) J Phys Chem 86:2232
16. Ju GZ, Chen DZ (1990) Int J Quant Chem 38:75
17. Ju GZ, Chen DZ (1989) Acta Chimica Sinica, Engl Ed 6:496
18. Isaacson AD, Truhlar DG, Rai SN, Steckler R, Honcock GC, Garrett BC, Redmon MT (1987) Computer Physics Communications 47:91
19. Kuppermann A (1981) in: Truhlar DG (ed) Potential energy surfaces and dynamics calculations. Plenum, London, NY, p 375
20. Broida M, Tamir M, Persky A (1986) Chem Phys 110:83
21. Persky A Broida M (1987) Chem Phys 114:85
22. Smith IWM (1980) Kinetics and Dynamics of Elementary Gas Reactions, Butterworths, London, p 100
23. Truhlar DG, Isaacson AD, Garrett BC (1985) in: Baer M (ed) Theory of chemical reaction dynamics, vol IV. CRC Press Inc, Boca Raton, FL, p 65
24. Schwenke DW, Tucker SC, Truhlar DG, Garrett BC (1989) J Chem Phys 90:3110
25. Polanyi JC (1972) Accounts Chem Res 5:161